Mesoscopically Periodic Photonic-Crystal Materials for Linear and Nonlinear Optics and Chemical Sensing

Sanford A. Asher, John Holtz, Jesse Weissman, and Guisheng Pan

Introduction

Over the past decade, we have been working to develop intelligent photonic-crystal materials with unique properties, which will be useful in a number of technological areas. These photonic-crystal materials utilize mesoscopically periodic arrays of spherical particles as their active optical elements and are easily fabricated chemically by the use of crystalline-colloidal-array (CCA) self-assembly techniques.

Crystalline colloidal arrays are mesoscopically periodic fluid materials, which efficiently diffract light meeting the Bragg condition.[1-4] These photonic-crystal materials consist of arrays of colloidal particles that self-assemble in solution into either face-centered-cubic (fcc) or body-centered-cubic (bcc) crystalline arrays[1,5] (Figure 1), with lattice constants in the mesoscale size range (50–500 nm). Just as atomic crystals diffract x-rays that meet the Bragg condition, CCAs diffract ultraviolet, visible, and near-infrared light, depending on the lattice spacing;[2-4] the diffraction phenomena resemble those of opals, which are close-packed arrays of monodisperse silica spheres.[6]

The CCA however can be prepared as macroscopically ordered arrays of non-close-packed spheres. This self-assembly is the result of electrostatic repulsions between colloidal particles, each of which has numerous charged surface functional groups. We have concentrated on the development of CCAs that diffract light in the visible spectral region and generally utilize colloidal particles of ~100-nm diameter.[7] These particles have thousands of surface charges, which result from the ionization of surface sulfonate groups. The nearest-neighbor distances are often >200 nm.

Photonic-Crystal Diffraction Devices

These bcc or fcc cubic arrays are well-ordered and the arrays strongly diffract light in the visible spectral region (Figure 2). All light meeting the Bragg condition is diffracted, whereas adjacent spectral regions freely transmit. We earlier demonstrated the use of these CCAs as narrow-band optical diffraction filters.[1c,3] We more recently developed methods[8,9] to solidify and stiffen these arrays by forming polymerized CCAs (PCCAs) that are fabricated by imbedding the CCA lattice into a hydrogel polyacrylamide network (Figure 3). These resulting solid photonic crystals can be prepared such that the acrylamide and the colloidal particles occupy a small percent of the sample volume, which consists mostly of water. The medium surrounding the spheres can be modified because other solvents can be diffused into the polymerized array to replace the water. Although the hydrogel-linked CCA undergoes swelling and shrinkage as the solvent medium is changed, the array ordering is maintained. Single-crystal films of this array can be prepared in which the (111) planes of the fcc lattice are well-oriented and parallel to the surface. Sunkara et al. at Oklahoma have more recently developed an alternative polymerization strategy for forming solidified CCA materials.[10]

Optically Nonlinear Photonic Crystals

We[11,12] as well as others[13] proposed that optically nonlinear photonic crystals could be fabricated using optically non-

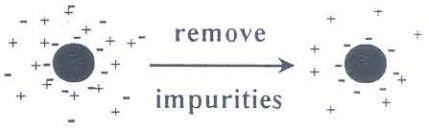

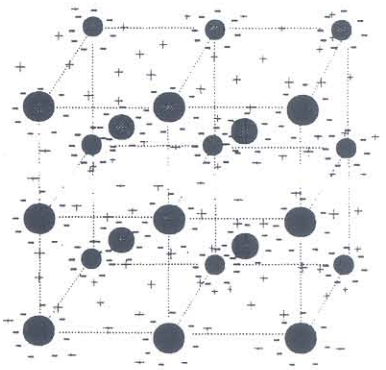

Figure 1. Crystalline colloidal array (CCA) composed of a body-centered-cubic lattice of negatively charged colloidal particles. The colloidal-particle charges derive from ionization of surface sulfonate groups. The counterions in the surrounding medium maintain the system net neutrality. In low-ionic-strength solutions, the electrostatic repulsions between colloidal particles cause the system to self-assemble into its lowest energy form.

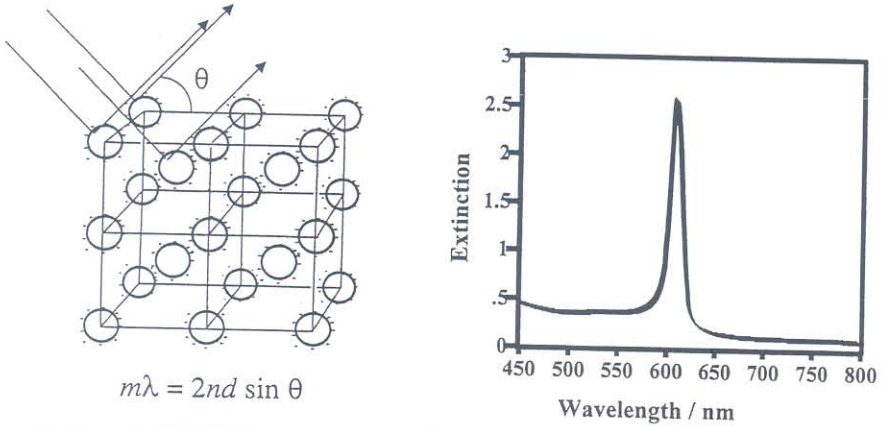

Figure 2. Transmission spectrum of a 200-μm-thick CCA formed from 242-nm-diameter poly(1H, 1H –heptafluorobutyl methacrylate) particles. The CCA structure was face-centered-cubic (fcc) and the array formed with the fcc (111) plane perpendicular to the incident light. Light meeting the Bragg condition is diffracted by the (111) planes according to Bragg's law where m is the order of diffraction, λ is the wavelength of incident light, n is the suspension refractive index, d is the interplanar spacing, and θ is the glancing angle between the incident light and the diffracting crystals.

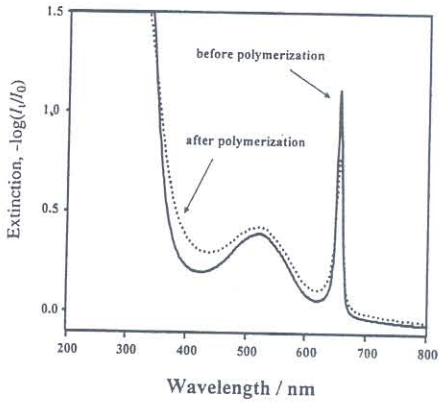

Figure 3. Transmission spectra of 155-nm-diameter poly(heptafluorobutyl methacrylate) CCA before and after solidification in a polyacrylamide hydrogel matrix. The colloidal particles have an absorbing dye covalently attached, and the transmission spectra show a ~520-nm absorption band for the dye and a ~650-nm peak from diffraction from the (111) planes of the fcc crystal. I_t and I_0 are the transmitted and incident intensities.

linear colloidal particles. One approach would make use of organic polymer spheres containing an absorbing dye. The composition of the medium would be adjusted such that the real part of the refractive index of the spheres is identical to that of the medium.[12c] Thus at low light intensities, the array would not diffract light that meets the Bragg condition. At high incident light intensities however, significant heating of the colloidal particles would occur, the temperature would increase, the refractive index would decrease, and the array would "pop up" to diffract light. We calculated that the switching time of these nonlinear photonic crystals could be ~5 ns for pulsed-laser sources.[12c]

We synthesized 138-nm-diameter monodisperse colloidal particles of heptafluorobutyl methacrylate and covalently attached an acylated Oil Blue N dye to these colloidal spheres.[14] These monodisperse highly charged fluorinated colloids have the lowest refractive index (n = 1.386) of any monodisperse colloid known. These fluorinated colloids were self-assembled into a CCA that was polymerized within an acrylamide hydrogel. Dimethyl sulfoxide was added to the mainly aqueous medium in order to adjust the medium refractive index to be either slightly above or slightly below that of the colloidal particles.

Diffraction by the array was monitored using the experimental apparatus shown in Figure 4. The 532-nm pump beam derived from a Coherent Inc. Infinity frequency doubled yttrium-aluminum-garnet laser.[5,6] The probe beam derived from a dye laser pumped by the 532-nm beam. The 3.5-ns duration pump and the probe beams were made coincident on

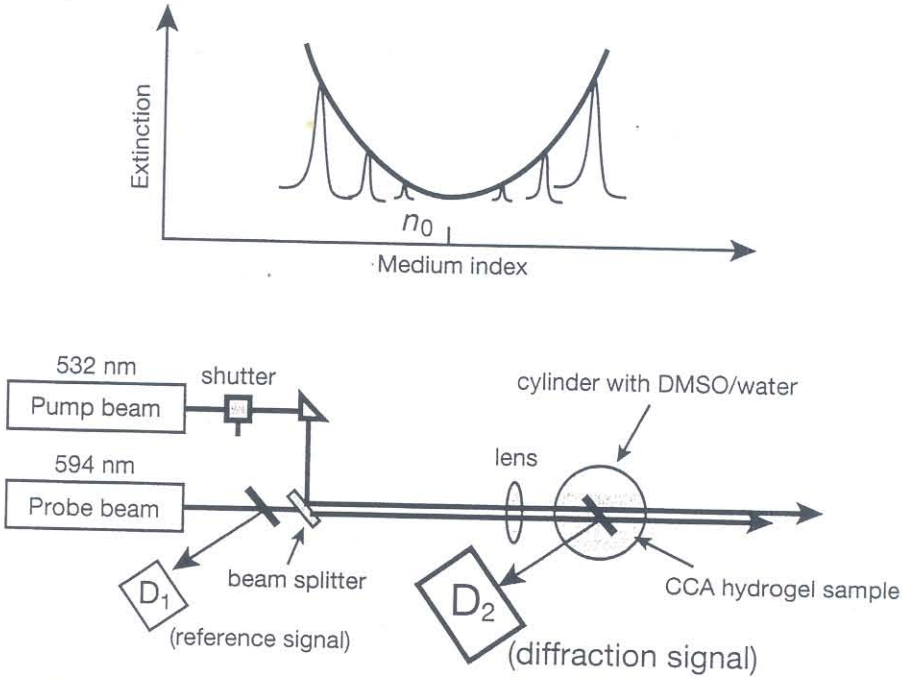

Figure 4. Schematic of the experimental apparatus for optical nonlinear diffraction measurements.[15,16] The extinction spectrum above shows the dependence of the Bragg diffraction efficiency on the refractive-index mismatch between the spheres and the medium.

the sample, but the probe beam was adjusted temporally such that it was delayed by ca. 2.5 ns compared to the pump beam. The relative angle of the sample to the probe beam was adjusted such that the Bragg condition was met. If the refractive indices were exactly matched, no diffraction would be observed in the absence of the pump beam. If the refractive index of the colloidal particles was adjusted to be slightly greater or less than that of the medium, a small fraction of the probe beam would diffract.

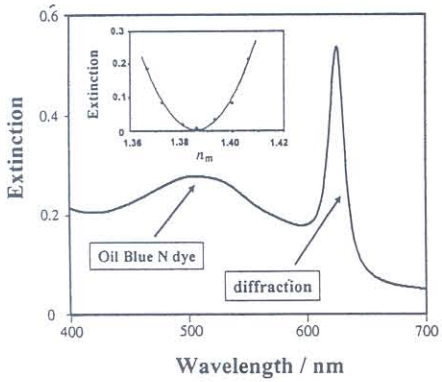

Figure 5. Extinction spectrum of dyed polymerized CCA (PCCA) of Figure 3 with an inset showing the diffraction intensity as a function of the refractive index of the medium. The real part of the refractive index is matched at n_m = 1.386—the value of the real part of the refractive index of the fluorinated colloid particles.

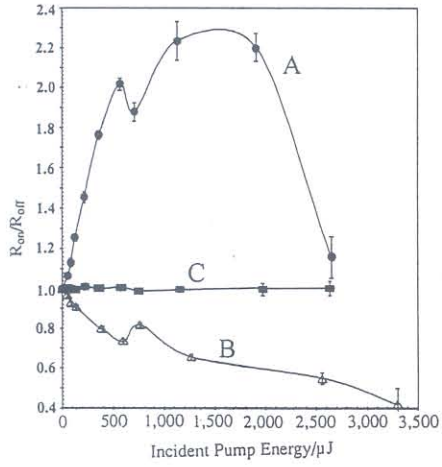

Figure 6. Pump-beam-energy dependence of Bragg-diffraction intensity. The relative value of Bragg-diffraction intensities (R_{on}/R_{off}) were monitored at various pump-beam energies. • is dyed CCA hydrogel in the medium of water and DMSO at n = 1.3908, △ is DMSO at n = 1.3813, and ■ is undyed CCA hydrogel in the medium at n = 1.3875.[15,16]

Figure 5 shows the extinction spectrum of a dyed CCA nonlinear photonic-crystal film measured at normal incidence.[14] The broad 520-nm band results from the colloidal particle dye absorption. The 640-nm peak results from the fcc (111)-plane Bragg diffraction. The film was oriented such that its normal made an angle of ~15° relative to the incident beam, such that light at the dye laser output at 594 nm would be diffracted onto the detector. Figure 6 shows a series of three measurements at which the medium has a refractive index of either 1.3813 or 1.3908—either below or above the sphere refractive index, or for a PCCA without dye. Figure 6 displays the relative value of the diffracted light intensity at various pump-energy values compared to that in the absence of the pump. As expected, if the colloid refractive index is below that of the medium, incident-beam heating further decreases the colloid refractive index below that of the medium and the diffracted intensity increases. In contrast if the colloid refractive index is above that of the medium, pump-beam heating decreases the refractive index toward that of the medium, and the diffraction decreases. Without dye no nonlinear response appears. Thus we experimentally observed the predicted nonlinear optical switching behavior from these CCAs.[15,16]

Time-dependent measurements show that this diffraction switching has a maximum at ~3 ns after the pump beam and that the nonlinear response is over in ~5 ns. Although we observed ns switching, the efficiency observed was small: ~2–3%. However we were able to independently demonstrate that the spheres heated up by the expected temperature based on the laser pulse and that this resulted in the expected refractive-index decrease. We recently demonstrated that this decreased diffraction efficiency results from residual disorder in the PCCA. We are now developing more ordered nonlinear PCCAs that will show much higher efficiency diffraction switching.

Thermally Tunable Photonic Crystals

We recently developed thermally tunable photonic crystals by utilizing the well known temperature-induced volume phase-transition properties of poly(*N*-isopropylacrylamide) (PNIPAM)[17–19] to create novel CCA photonic crystals with variable sphere sizes and variable array periodicities.[20] In water below ~30°C, PNIPAM is hydrated and swollen. When heated above its lower critical solution temperature (~32°C), it undergoes a reversible volume phase transition to a collapsed, dehydrated

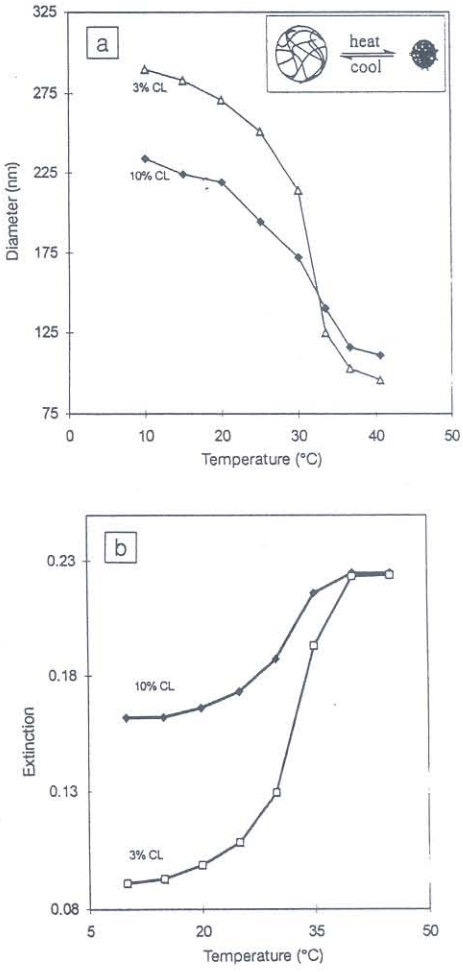

Figure 7. Temperature dependence of the poly(N-isopropylacrylamide) (PNIPAM) colloid diameter and turbidity. (a) The diameter of two PNIPAM colloid particles of 3% and 10% crosslinking was determined by quasielastic light scattering. (b) The temperature dependence of the turbidity was measured for a disordered dilute dispersion by measuring light transmission through a 1.0-cm path-length quartz cell. The light scattering increases as the particle becomes more compact because of its increased refractive-index mismatch from the aqueous medium.[20]

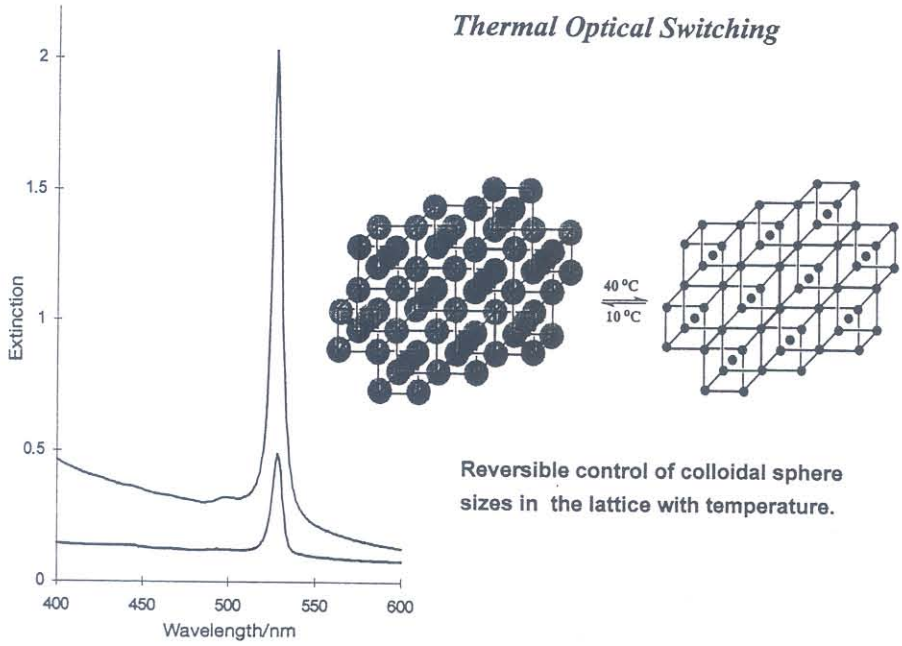

Figure 8. Diffraction from a CCA of PNIPAM spheres at 10°C and at 40°C. The spectra were recorded using an ultraviolet (uv)-visible near infrared (ir) spectrophotometer (Perkin Elmer λ-9). The dispersion was contained in a 1.0-mm quartz cuvette oriented at normal incidence to the incident beam. The observed diffraction switching behavior was reversible; these spectra were recorded after the seventh consecutive heat-cool cycle. Inset: Representation of the temperature switching between a swollen sphere array below the phase-transition temperature and an identical compact sphere array above the transition (adapted from Reference 20).

state. The temperature increase causes the polymer to expel water and shrink into a more hydrophobic polymer state.

We developed a synthesis of monodisperse, highly charged colloidal particles of PNIPAM, the diameter of which depends on temperature.[20] *N*-isopropylacrylamide was polymerized with the ionic comonomer 2-acrylamido-2-methyl-1-propane sulfonic acid to increase the colloid surface charge that facilitates CCA self-assembly. Figure 7 shows the temperature dependence of the colloidal sphere diameter. The diameter decreases from ~300 nm at 10°C to ~100 nm at 40°C for particles with 3% crosslinking. The change in sphere size impacts the scattering power as is observed by the turbidity measurement of Figure 7. Counterintuitively the smaller spheres scatter more than the larger spheres; however this is explained by the larger refractive-index mismatch for the shrunken spheres at the higher temperatures.

These PNIPAM colloids self-assemble in deionized water to form CCA photonic crystals both above and below the polymer phase-transition temperature. The ordered array diffracts light almost following Bragg's diffraction law (but not exactly as shown elsewhere[4]):

$$m\lambda = 2nd \sin\theta \qquad (1)$$

where m is the order of diffraction, λ is the wavelength of incident light, n is the suspension refractive index, d is the interplanar spacing, and θ is the glancing angle between the incident light and the diffracting crystal planes,[4] which are oriented parallel to the crystal surface in the CCA we prepare. Figure 8 shows the resulting extinction spectra of a PNIPAM CCA photonic crystal at 10°C and 40°C. At low temperatures, the CCA particles are highly swollen—almost touching—and diffract weakly because of their small refractive-index mismatch. Above the phase-transition temperature, these particles become compact, increase their refractive index, and diffract nearly all incident light at the Bragg wavelength. The temperature change does not affect the lattice spacing. This photonic crystal acts as a thermally controlled optical filter.

In addition we used a similar concept[20] to fabricate wavelength-tunable photonic crystals using a PNIPAM gel to control the periodicity of the CCA. We polymerized a CCA of polystyrene spheres in PNIPAM. This PCCA shrinks and swells continuously and reversibly between 10°C and 35°C; the embedded PS sphere array shrinks and swells as well, changing the lattice spacing and thus the diffracted wavelength (Figure 9).

This PCCA photonic crystal functions as a tunable optical filter; the diffraction wavelength can be altered by varying either the temperature or the angle of incidence. At a fixed angle to the incident beam, this PCCA acts as a tunable wavelength reflector. The width and height of

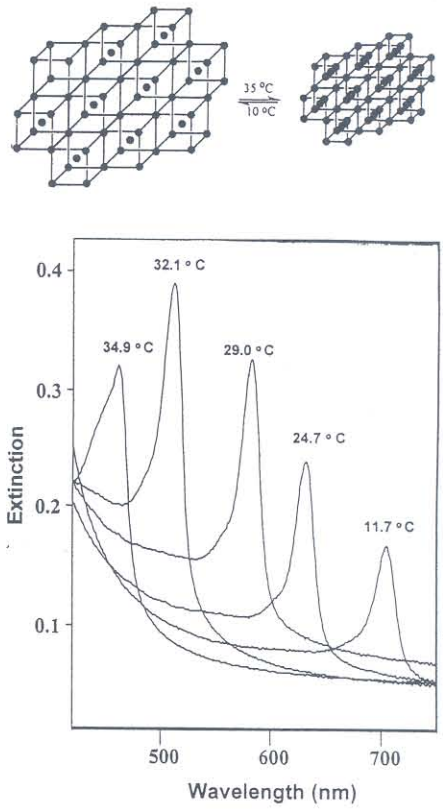

Figure 9. Temperature tuning of Bragg diffraction from a 125-mm-thick PCCA film of 99-nm polystyrene spheres embedded in a PNIPAM gel. The diffraction wavelength shift results from the temperature-induced volume change of the gel, which alters the lattice spacing. Spectra were recorded in an ultraviolet-visible near-ir spectrophotometer with the sample placed normal to the incident light beam (adapted from Reference 20).

the diffraction peak can be easily controlled through the selection of colloidal particles of different sizes and refractive indices or by making different-thickness PCCA films.[20] The tuning range of this device can be widened or narrowed by synthesizing PCCA films with lower or higher crosslinking concentrations. The ability to dynamically control the diffraction wavelength makes these materials useful for display device applications.

Chemical-Sensing Photonic Crystals

In the PCCA materials, the CCA lattice is locked in place by the surrounding hydrogel. As observed for the thermally responsive PCCA, the lattice spacing changes in proportion to changes in the dimension of the hydrogel. We used this concept to develop a series of chemical-sensing photonic crystals in which the presence of different analyte concentrations drives hydrogel volume changes, which are simply detected by shifts in the diffracted wavelength (Figure 10).

We fabricated an Intelligent PCCA (IPCCA) sensitive to Pb^{2+}, Ba^{2+}, and K^+ by copolymerizing 4-acryloylaminobenzo-18-crown-6 into the PCCA. This crown ether selectively complexes Pb^{2+}, Ba^{2+}, and K^+.[21,22] The crown-ether binding of these particular cations localizes charges onto the gel network. The gel swelling mainly results from an increased osmotic pressure within the gel due to a Donnan potential arising from the mobile counterions to the crown-ether bound cations.[22] The cation binding forms a polyelectrolyte hydrogel, for which the charge state is only determined by the number of cations bound; the degree of swelling of polyelectrolyte gels increases with the number of covalently attached charged groups.

Figure 11 shows that the IPCCA volume and diffraction wavelength monotonically increases with increasing Pb^{2+} concentrations between 0.1 μM (~20 ppb) and 10 mM (~2,000 ppm) at moderate ionic strengths of noninterfering electrolytes (<1 mM LiCl, for example); the shift in the IPCCA diffraction induced by 20-μM $Pb(CH_3COO)_2$ (4 ppm) is easily visible to the naked eye. The hydrogel volume maximum occurs at ~10 mM Pb^{2+} at which point the crown ethers become saturated. At higher Pb^{2+} concentrations, the gel begins to shrink because of the decrease in the Donnan osmotic pressure at higher ionic strengths. The swelling is reversible; the diffraction reverts to its original wavelength when Pb^{2+} exchanges out through soaking for a few minutes in deionized water.

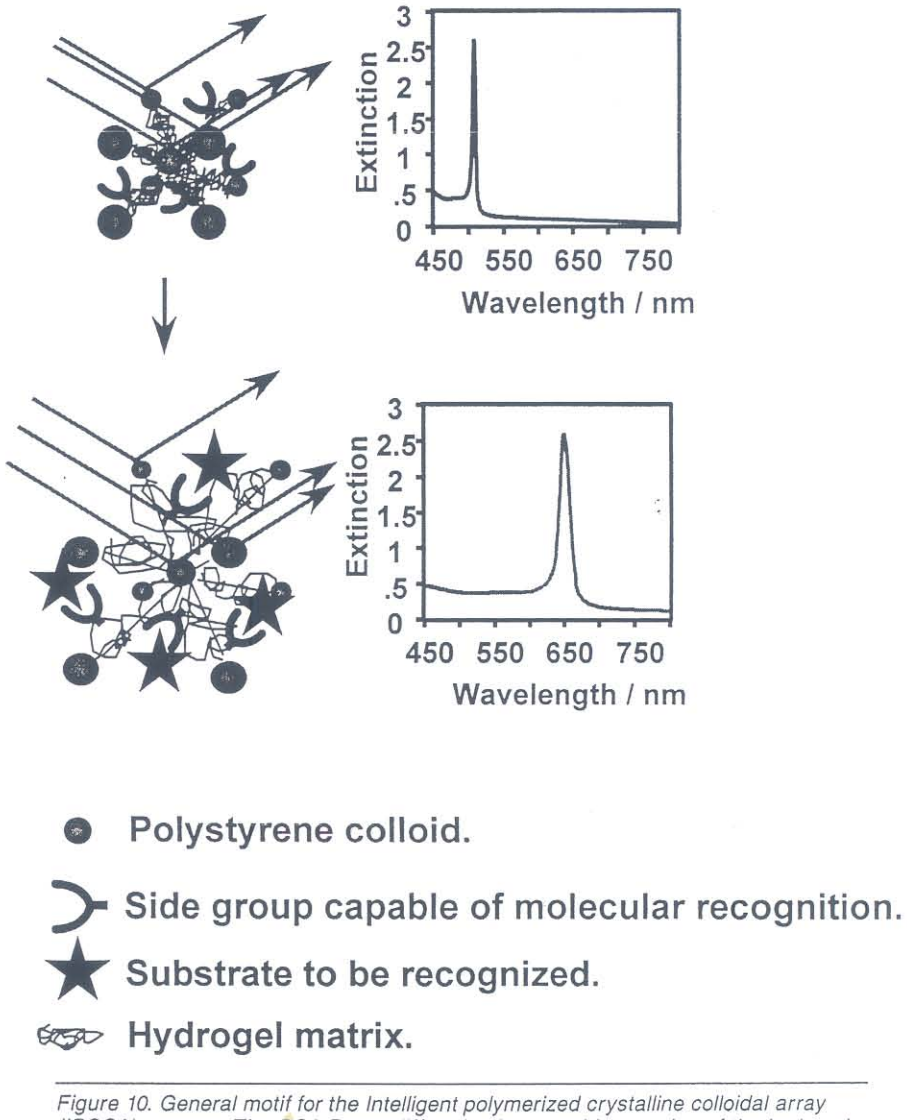

Figure 10. General motif for the Intelligent polymerized crystalline colloidal array (IPCCA) sensors. The CCA Bragg diffraction is a sensitive monitor of the hydrogel volume change induced by the interaction or binding of the molecular recognition agent to a substrate. In principle any molecular recognition agent can be attached to the hydrogel polymer to produce an IPCCA sensor.

The selectivity of the IPCCA sensor volume response is determined by the selectivity of the molecular recognition agent. For example the 18-crown-6 complex shows log K values (K is the equilibrium binding constant) of 3.87 and 4.27 for Ba^{2+} and Pb^{2+}, respectively. Thus Ba^{2+} swells the PCCA almost identically to Pb^{2+}, making it the major interfering species. K^+ competes with Pb^{2+} for binding only for K^+ concentrations ~200-fold larger than that of the Pb^{2+}, whereas a 2,000-fold excess of Na^+ is required to compete with Pb^{2+} binding.

Ions that are not complexed by the crown ether only interfere with the IPCCA Pb^{2+} response at relatively high concentrations, because of their ionic strength impact on decreasing the Donnan osmotic pressure. For example 1-mM concentrations of Li^+ and H^+ do not affect the response to 1 μM Pb^{2+}.

We also fabricated a photonic-crystal glucose sensor[21,22] by attaching the enzyme glucose oxidase (GOx) to a PCCA of polystyrene colloids. We hydrolyzed the PCCA, biotinylated it, and attached ~20 mg of avidinated GOx per cm^3 of PCCA—giving a ~25-nm spacing between enzymes. Glucose solutions prepared in air cause the IPCCA to swell and result in the diffraction redshifts as

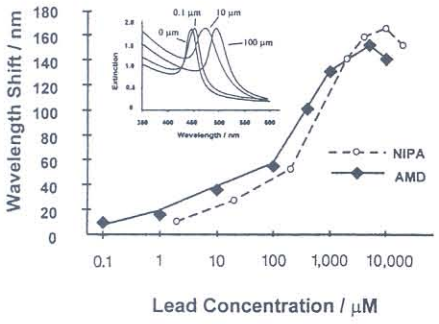

Figure 11. Dependence of diffraction on $Pb(CH_3COO)_2$ concentration. Inset shows dependence of the extinction spectra of the IPCCA Pb^{2+} sensor as measured at normal incidence during immersion of the IPCCA in different Pb^{2+} solutions by using a Perkin-Elmer Lambda-9 UV-Visible spectrophotometer.

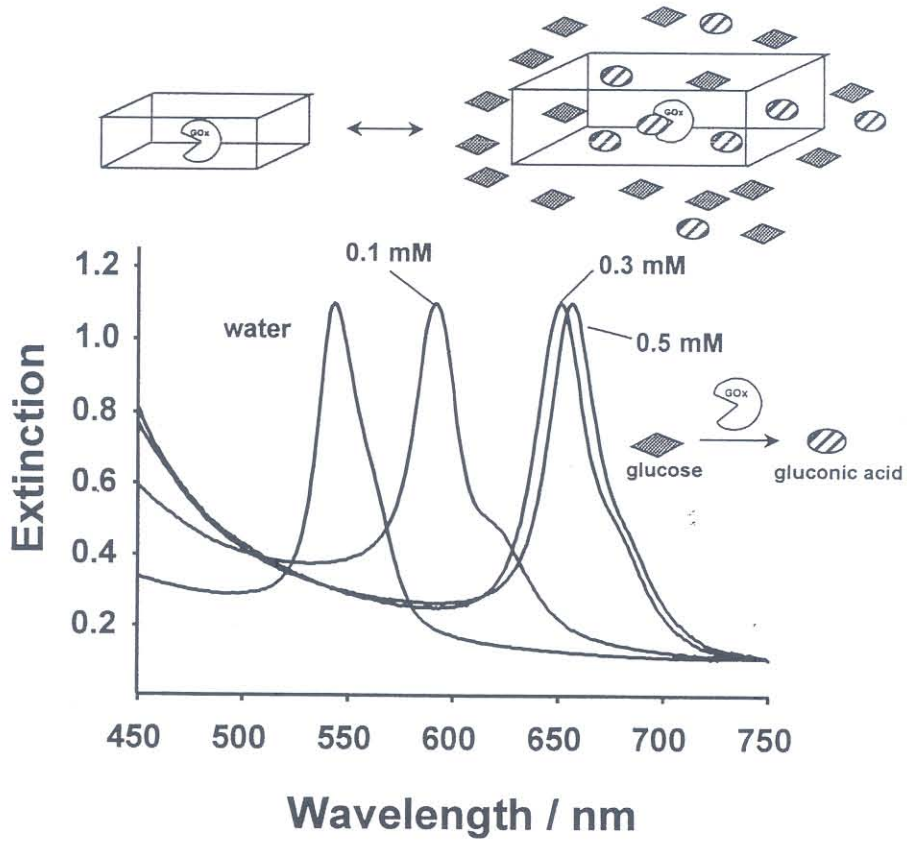

Figure 12. Visible extinction spectra showing the glucose-concentration dependence of diffraction for the 125-μm-thick PCCA glucose sensor. The IPCCA expands between 0.1-mM to 0.5-mM glucose.

shown in Figure 12. No response occurs for similar concentrations of sucrose or mannose, because of the enzyme selectivity. The swelling saturates above 0.5-mM glucose because of formation of a steady state for the conversion of glucose to gluconic acid, coupled with the reoxidation of the GOx by dissolved oxygen. This IPCCA returns to its original diffraction wavelength after removal from glucose.

The IPCCA swelling results from formation of a reduced flavin anion upon glucose turnover. The oxidized flavin is uncharged at neutral pH; however the reduced flavin is anionic at pH 7. The reduced flavin is reoxidized by O_2.

The anionic, reduced-flavin steady-state concentration depends upon both the concentration of glucose and of dissolved oxygen. In the absence of oxidants, the gel responds to even 10^{-12}-M glucose concentrations;[21,22] the diffraction redshifts 8 nm within 30 min if the solution is stirred. At constant glucose concentrations, the number of anionic, reduced flavins depends upon the dissolved-oxygen concentration (Figure 13). Reoxidation of the flavin shrinks the IPCCA because of the reduced number of hydrogel charges.

These intelligent IPCCA photonic crystals represent a new chemical-sensing motif that can be tailored to detect a host of analytes. An important feature of these photonic-crystal chemical-sensing materials is that the diffraction-wavelength shifts make it easy to visually monitor the analyte concentration. For more quantitative measurements, this material can be used as the sensing element of an optrode. We demonstrated that we could put a small sensing film on the end of an optical fiber.[22] By launching light down the fiber and measuring the spectrum of the light diffracted back into the fiber, we remotely monitored the diffracted wavelength to determine the analyte concentration.

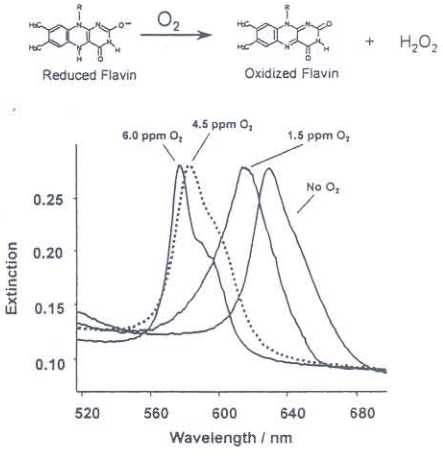

Figure 13. Extinction spectra of the PCCA glucose sensor in 0.2-mM glucose with varying O_2 concentrations. The sensor diffracted at 545 nm in the absence of glucose.

Conclusions

These mesoscale periodic materials are a new class of photonic materials that can be fabricated to be responsive to their environment. The uniqueness of these materials is that they originate through the self-assembly of a soft material, a colloidal dispersion. We see a bright future for this approach. The approach for applying soft materials for technology is a natural evolution of materials science that has progressed from the use of existing natural materials to the development of higher performance materials such as metals and ceramics. The utilization of

soft materials in technology has just recently begun; the most obvious example is the use of liquid crystals for display applications. We look forward to future applications of the soft CCA photonic-crystal materials discussed here.

Acknowledgments

This work was supported by the Office of Naval Research Grant No. N00014-94-1-0592, AASERT Grant No. F 49620-94-1-0268, and the National Science Foundation Grant No. CHE-9633561.

References

1. The physics of crystalline colloidal array ordering and phase transitions is quite extensive with a few hundred references over the last 30 years. The following recent publications are excellent reviews: (a) D. Thirumalai, *J. Phys. Chem.* **93** (1989) p. 5637; (b) A.M. Walsh and R.D. Coalson, *J. Chem. Phys.* **100** (1994) p. 1559; (c) S.A. Asher, U.S. Patent Nos. 4,627,689, 4,632,517 (1986), and 5,452,123 (1995); (d) P.A. Hiltner and I.M. Krieger, *J. Phys. Chem.* **73** (1969) p. 2386; (e) N.A. Clark, A.J. Hurd, and B.J. Ackerson, *Nature* **281** (1979) p. 57; (f) S. Alexander, P.M. Chaikin, P. Grant, G.J. Morales, P. Pincus, and D. Hone, *J. Chem. Phys.* **80** (11) (1984) p. 5776; (g) Y. Monovoukas and A.P. Gast, *J. Colloid I. Sci.* **128** (2) (1989) p. 533; (h) I.M. Krieger and F.M. O'Neill, *J. Am. Chem. Soc.* **90** (1968) p. 3114; (i) V.W. Luck, M. Klein, and H. Wesslau, *Ber. Bunsenges. Phys. Chem.* **67** (1963) p. 75; (j) D. Hone, S. Alexander, P.M. Chaikin, and P. Pincus, *J. Chem. Phys.* **79** (1983) p. 1474.
2. R.J. Carlson and S.A. Asher, *Appl. Spectrosc.* **38** (1984) p. 297.
3. (a) P.L. Flaugh, S.E. O'Donnell, and S.A. Asher, *ibid.* p. 847; (b) S.A. Asher, P.L. Flaugh, and G. Washinger, *Spectroscopy* **1** (1986) p. 26.
4. P.A. Rundquist, P. Photinos, S. Jagannathan, and S.A. Asher, *J. Chem. Phys.* **91** (1989) p. 4932.
5. J.C. Zahorchak, R. Kesavamoorthy, R.D. Coalson, and S.A. Asher, *ibid.* **96** (1982) p. 6874.
6. J.V. Sanders, *Nature* **204** (1964) p. 1151.
7. (a) P.A. Rundquist, S. Jagannathan, R. Kesavamoorthy, C. Brnardic, S. Xu, and S.A. Asher, *J. Chem. Phys.* **94** (1981) p. 711. (b) R. Kesavamoorthy, S. Jagannathan, P.A. Rundquist, and S.A. Asher, *ibid.* p. 5172; (c) P.A. Rundquist, R. Kesavamooorthy, S. Jagannathan, and S.A. Asher, *ibid.* **95** p. 1249; (d) *ibid.* p. 8546.
8. S.A. Asher, J. Holtz, L. Liu, and Z. Wu, *J. Am. Chem. Soc.* **116** (1994) p. 4997.
9. (a) S.A. Asher and S. Jagannathan, U.S. Patent No. 5,281,370 (1994); (b) G. Haacke, H.P. Panzer, L.G. Magliocco, and S.A. Asher, U.S. Patent No. 5,266,238 (1993).
10. (a) H.B. Sunkara, J.M. Jethmalani, and W.T. Ford, *Chem. Mater.* **6** (1994) p. 362; (b) *ibid., ACS Symp. Ser.* **585** (1995) p. 181.
11. (a) S.A. Asher, S-Y. Chang, A. Tse, L. Liu, G. Pan, Z. Wu, and P. Li, in *Materials for Optical Limiting*, edited by R. Crane, K. Lewis, E. Van Stryland, and M. Khoshnevisan (Mater. Res. Soc. Symp. Proc. **374**, Pittsburgh, 1995) p. 305; (b) S.A. Asher, R. Kesavamoorthy, S. Jagannathan, and P. Rundquist, in *Proc. SPIE Nonlinear Optics III*, vol. 1626 (Society of Photo-Instrumentation Engineers, 1992) p. 238; (c) S.A. Asher, S-Y. Chang, S. Jagannathan, R. Kesavamoorthy, and G. Pan, U.S. Patent No. 5,452,123 (1995).
12. (a) S-Y. Chang, L. Liu, and S.A. Asher, in *Better Ceramics Through Chemistry VI*, edited by A.K. Cheetham, C.J. Brinker, M.L. Mecartney, and C. Sanchez (Mater. Res. Soc. Symp. Proc. **346**, Pittsburgh, 1994) p. 875; (b) *ibid., J. Am. Chem. Soc.* **116**, (1994) p. 6739; (c) R. Kesavamoorthy, M.S. Super, and S.A. Asher, *J. Appl. Phys.* **71** (1992) p. 1116.
13. R.J. Spry and D.J. Kosan, *Appl. Spectrosc.* **40** (1986) p. 782.
14. G. Pan, A.S. Tse, R. Kesavomoorthy, and S.A. Asher, *J. Am. Chem. Soc.* **120** (1998) p. 6518.
15. G. Pan, R. Kesavomoorthy, and S.A. Asher, *Phys. Rev. Lett.* **78** (1997) p. 3860.
16. *Ibid., J. Am. Chem. Soc.* **120** (1998) p. 6525.
17. Y. Hirokawa and T. Tanaka, *J. Chem. Phys.* **81** (1984) p. 6379.
18. H.G. Schild, *Prog. Polym. Sci.* **17** (1992) p. 163.
19. X.S. Wu, A.S. Hoffman, and P. Yager, *J. Polym. Sci. Polym. Chem.* **A30** (1992) p. 2121.
20. J. Weissman, H.B. Sunkara, A.S. Tse, and S.A. Asher, *Science* **274** (1996) p. 959.
21. J.H. Holtz and S.A. Asher, *Nature* **389** (1997) p. 829.
22. J.H. Holtz, J.S.W. Holtz, C.H. Munro, and S.A. Asher, *Anal. Chem.* **70** (1998) p. 780. □

Why settle for fine micron size powders when nanopowders are 100x finer?

When it comes to thinking small particles, no one is bigger than Nanomaterials Research Corporation. At NRC, four years of nano-engineering has resulted in a patented process for affordable, bulk production of nanoscale fine powders.

To make a quantum change in products you make, make a quantum change in materials you use.

Whether you need dispersable nanostructured particles of magnetic, dielectric, or conducting nitrides, borides, carbides, oxides, alloys or speciality compositions–or you'd like to know how these nanoscale materials can be quickly integrated into your products–our proprietary technology and talented team can help you.

For more information on how Nanomaterials can help you reduce your manufacturing costs, re-engineer your existing products or explore your technology frontier–please call or fax us.

2620 Trade Center Ave.
Longmont, CO 80503, USA
Voice: 303-702-1672
Fax: 303-702-1682
www.nrcorp.com

NANOMATERIALS
RESEARCH CORPORATION

Circle No. 14 on Reader Service Card.